



Universiteit
Leiden
The Netherlands

MRI of diffuse-type tenosynovial giant cell tumour in the knee: a guide for diagnosis and treatment response assessment

Spierenburg, G.; Ballesteros, C.S.; Stoel, B.C.; Canete, A.N.; Gelderblom, H.; Sande, M.A.J. van de; Langevelde, K. van

Citation

Spierenburg, G., Ballesteros, C. S., Stoel, B. C., Canete, A. N., Gelderblom, H., Sande, M. A. J. van de, & Langevelde, K. van. (2023). MRI of diffuse-type tenosynovial giant cell tumour in the knee: a guide for diagnosis and treatment response assessment. *Insights Into Imaging*, 14(1). doi:10.1186/s13244-023-01367-z

Version: Publisher's Version

License: [Creative Commons CC BY 4.0 license](https://creativecommons.org/licenses/by/4.0/)

Downloaded from: <https://hdl.handle.net/1887/3590556>


Note: To cite this publication please use the final published version (if applicable).

EDUCATIONAL REVIEW

Open Access



MRI of diffuse-type tenosynovial giant cell tumour in the knee: a guide for diagnosis and treatment response assessment

Geert Spierenburg^{1*} , Carlos Suevos Ballesteros², Berend C. Stoel³, Ana Navas Cañete⁴, Hans Gelderblom⁵, Michiel A. J. van de Sande¹ and Kirsten van Langevelde⁴

Abstract

Tenosynovial giant cell tumour (TGCT) is a rare soft-tissue tumour originating from synovial lining of joints, bursae and tendon sheaths. The tumour comprises two subtypes: the localised-type (L-TGCT) is characterised by a single, well-defined lesion, whereas the diffuse-type (D-TGCT) consists of multiple lesions without clear margins. D-TGCT was previously known as pigmented villonodular synovitis. Although benign, TGCT can behave locally aggressive, especially the diffuse-type. Magnetic resonance imaging (MRI) is the modality of choice to diagnose TGCT and discriminate between subtypes. MRI can also provide a preoperative map before synovectomy, the mainstay of treatment. Finally, since the arrival of colony-stimulating factor 1-receptor inhibitors, a novel systemic therapy for D-TGCT patients with relapsed or inoperable disease, MRI is key in assessing treatment response. As recurrence after treatment of D-TGCT occurs more often than in L-TGCT, follow-up imaging plays an important role in D-TGCT. Reading follow-up MRIs of these diffuse synovial tumours may be a daunting task. Therefore, this educational review focuses on MRI findings in D-TGCT of the knee, which represents the most involved joint site (approximately 70% of patients). We aim to provide a systematic approach to assess the knee synovial recesses, highlight D-TGCT imaging findings, and combine these into a structured report. In addition, differential diagnoses mimicking D-TGCT, potential pitfalls and evaluation of tumour response following systemic therapies are discussed. Finally, we propose automated volumetric quantification of D-TGCT as the next step in quantitative treatment response assessment as an alternative to current radiological assessment criteria.

Key Points

- TGCT is categorised according to its site of involvement and growth pattern.
- D-TGCT is characterised by irregular synovial proliferation infiltrating multiple synovial knee recesses.
- Systematic MRI approach is provided for preoperative and systemic treatment response assessment.
- An overview of synovial knee recesses guides the radiologist in assessing blind spots.
- Machine learning-based tumour segmentation may be applied to assess D-TGCT tumour volume in the near future, so that treatment response assessment can be quantified and improved by artificial intelligence.

*Correspondence:
Geert Spierenburg
G.Spierenburg@lumc.nl
Full list of author information is available at the end of the article

Keywords Tenosynovial giant cell tumour, Diffuse-type TGCT, Magnetic resonance imaging, Colony-stimulating factor 1, 3D segmentation

Introduction

Tenosynovial giant cell tumour (TGCT) is a fibro-histiocytic soft-tissue tumour that involves anatomical structures covered by a synovial membrane (joints, bursae and tendon sheaths). It can also affect extra-synovial locations, such as subcutaneous and intramuscular lesions [1]. Common symptoms are pain, swelling, stiffness, and limited function, leading to decreased quality of life [2].

TGCT can be classified according to its site (intra- and extra-articular) and growth pattern [3]. In the 2013 World Health Organisation classification of soft tissue and bone tumours, localised-type (L-TGCT) and diffuse-type (D-TGCT) replaced the terminology “giant cell tumour of the tendon sheath” and “pigmented villonodular synovitis”, respectively [1]. There is no clear histological distinction between both subtypes, therefore, diagnosis is based on radiological diagnosis and clinical presentation [4]. TGCT is a rare neoplasm with incidence rates of 45 and 5 per million person-years for L-TGCT and D-TGCT, respectively. TGCT has a female predilection (♀:♂; 2:1) and affects a relatively young patient group mainly aged between 30 and 50 years, although it can occur at any age [5, 6].

L-TGCT occurs in an extra-articular location in 90% of cases, involving tendon sheaths of the volar aspect of fingers (85%), followed by foot and knee locations (15%) [7]. These tumours primarily present as painless soft-tissue masses without joint dysfunction. The diffuse type originates predominantly in the intra-articular space of large joints such as the knee (70%) followed by the hip (15%) but often extends extra-articular [5]. The extra-articular D-TGCT form is mostly a secondary extension of intra-articular disease [8]. D-TGCT tends to present with chronic joint pain and swelling, often with progressive secondary osteoarthritis [2, 9]. D-TGCT represents a monoarticular disease, which means that in case of polyarticular involvement with similar MRI appearance, other diagnoses should be considered, such as gout, haemophilic or amyloid arthropathy.

TGCT subtypes share a common underlying pathogenesis, mainly related to a Colony-Stimulating Factor 1 (*CSF1*) translocation resulting in *CSF1* overexpression. *CSF1* overexpression causes an increase in neoplastic cells by binding to *CSF1*-receptors (*CSF1R*) and accumulating *CSF1R* presenting cells [10]. Histologically, TGCT shows an infiltrative growth pattern and comprises

mononuclear cells, multinuclear osteoclast-like giant cells, macrophages and stromal hyalinization. Also, hemosiderin depositions are frequently observed [1].

MRI is the imaging modality of choice for diagnosing and evaluating disease severity [11]. It gives insight into areas that are not amenable for arthroscopic evaluation. Thereby, MRI can provide a preoperative map of D-TGCT localisations to evaluate common blind spots before open synovectomy [8]. Achieving complete resection can be challenging, especially in extensive tumour growth. Incomplete resections are associated with a higher chance of tumour relapse [12, 13]. Other treatment modalities such as radiosynoviorthesis or external beam radiotherapy have been used to reduce relapse rates. However, evidence regarding the efficacy of these treatments is scarce [14, 15]. Furthermore, the role of radiotherapy for TGCT remains controversial because it may result in complications such as osteoarthritis in a young patient population [13]. With the arrival of *CSF1R*-inhibitors, a novel systemic therapy for D-TGCT patients not amenable to surgery, MRI is essential to select and follow-up on target lesions [16, 17].

In this educational review, we demonstrate the imaging features of D-TGCT and highlight blind spots and potential pitfalls on MRI.

Imaging features of D-TGCT

Radiography

Conventional radiography provides a first modality to assess osteoarticular complaints of the knee. Radiographs of the knee in D-TGCT are often normal, although features of osteoarthritis may be present, such as osteophytes, joint space narrowing and subchondral sclerosis. Pressure erosions may occur on both articular joint surfaces in advanced stages, especially in joints with limited volume and joint space, such as the ankle, hip and shoulder [9]. In the knee, erosions have been described on radiographs in up to 30% of patients [18].

The presence of (peri)articular soft-tissue calcifications pleads against the diagnosis of D-TGCT and differential diagnoses such as gout or synovial chondromatosis should be considered [19].

Ultrasound

Ultrasound is not part of the standard diagnostic workup of D-TGCT; however, it can be helpful in performing image-guided biopsies [20]. Appearance of D-TGCT has

been described as hypoechoic irregular synovial thickening along with heterogeneous joint effusion and hyperemia, although these findings are non-specific and may be found in other types of diffuse synovitis [21]. In addition, ultrasound does not provide the necessary information and correct evaluation of the areas that should be carefully scrutinised and reported when evaluating D-TGCT.

MRI

MRI is the modality of choice to diagnose D-TGCT. The scanning protocol applied at our tertiary referral centre for bone and soft tissue tumours (3 Tesla, Ingenia, Philips, Eindhoven, The Netherlands) is shown in Additional file 1: Table S1. A gradient-echo sequence may be beneficial for detecting hemosiderin related to tumour bleeding. Intravenous gadolinium contrast aids in tumour

detection and is helpful for follow-up after synovectomy. TGCT can present with variable MRI appearances given its heterogeneous histological composition and the variety in growth patterns (intra- and/or extra-articular) [3].

D-TGCT findings include irregular synovial thickening (>5 mm), typically described as “frond-like” with villous or nodular morphology [3]. This synovial proliferation tends to engulf associated reactive joint effusion resulting in multiloculated thick-walled trapped cystic masses, especially seen in the subgastrocnemius synovial recesses and Baker’s cysts [18].

D-TGCT intra-articular forms are likely to spread diffusely, developing a multicompartmental growth pattern involving at least two contiguous intra-articular synovial recesses. In the knee, several recesses may be involved, as illustrated in the detailed description of Fig. 1.

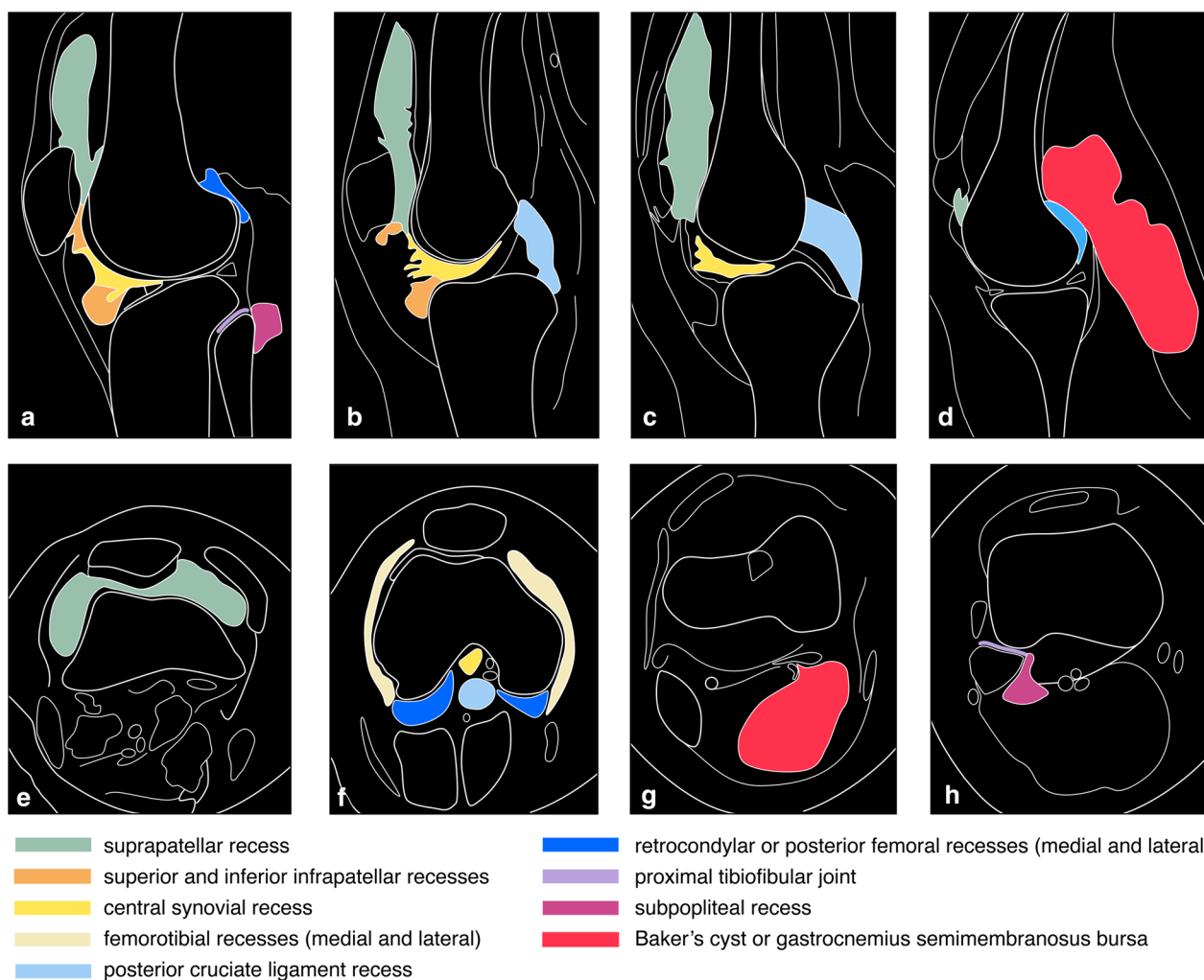


Fig. 1 Schematic overview of synovial recesses in the knee. **a–d** Sagittal drawings from lateral (**a**) to medial (**d**). **e–h** axial drawings from superior (**e**) to inferior (**h**)

D-TGCT's extra-articular growth pattern mainly occurs secondary to intra-articular extension through transcapsular fenestrations [8]. Mastboom et al. defined extra-articular extension as TGCT involvement outside the synovial lining of the joint. Furthermore, cartilage invasion, cortical bone erosions, muscular/tendinous, ligament and neurovascular involvement were proposed as parameters that determine the severity of D-TGCT [22]. In the knee, tibial nerve encasement is rare but may be symptomatic. D-TGCT may extend into femoral and tibial medullary tunnels in patients with anterior cruciate ligament (ACL) reconstruction.

D-TGCT signal intensity is heterogeneous. T1-weighted imaging (T1-WI) shows a hypointense to iso-intense signal, whereas fluid-sensitive sequences show a hyperintense signal with foci of low signal intensity corresponding to hemosiderin in the tumour (Fig. 2). D-TGCT is prone to bleeding (bleeding is more common than in L-TGCT), and therefore hemarthrosis is a common finding expressed as low signal intensity on both T1-WI and fluid-sensitive sequences. Haemorrhage constitutes a classic D-TGCT imaging hallmark mostly detected as blooming on gradient echo (GRE) images. This imaging feature has been described as pathognomonic to suggest TGCT diagnosis, but its absence does not exclude TGCT [23]. Blooming is a paramagnetic susceptibility artefact secondary to hemosiderin deposition defined as enlargement and disproportionately lower signal intensity of blood deposits on GRE images compared to spin-echo (SE) sequences (Fig. 3). Scout GRE acquisitions should be employed cautiously in the search for blooming owing to high false-negative rates [23]. Diffusion-weighted images (DWI) can be deceptive because TGCT (both localised and diffuse subtypes) depict intrinsically low apparent diffusion coefficient (ADC) values due to hemosiderin deposits [24]. D-TGCT shows avid heterogeneous enhancement. From dynamic post-contrast imaging (perfusion), a time-intensity curve can be obtained showing rapid early enhancement with a plateau phase (Fig. 2) [25].

Areas of intralesional fat with high signal intensity on T1-WI related to deposition of lipid-laden macrophages (xanthoma cells) are a classic feature of D-TGCT, however, this finding is uncommon [3, 23]. This feature may represent entrapped fronds of perisynovial fat or sub-synovial fat metaplasia as a reactive process to chronic TGCT, similar to lipoma arborescens in rheumatoid or psoriatic arthritis.

Differential diagnoses

Gout tophi can present as both intra- and extra-articular or peri-articular nodules. Typical locations such as the subcutaneous fat or within the distal quadriceps or

proximal patellar tendon can help distinguish gout from D-TGCT [26]. Gout and amyloidosis are soft-tissue masses appearing hypointense on T2 sequences, which can be intra-articular, mimicking TGCT (Fig. 4) [27]. Radiographs may be helpful to assess soft tissue calcifications, and dual-energy computed tomography (CT) may be performed to prove the presence of monosodium urate crystals in gout [28].

Synovial chondromatosis can present either as multiple round bodies similar in size and shape with a “snowstorm” or “cobblestone” pattern and a variable degree of calcification (85% is calcified) or coalesce into multiple intra-articular synovial masses (Fig. 5). The presence of calcification or metaplastic cartilage excludes the diagnosis of TGCT [19].

Lipoma arborescens is a chronic, slow-growing, intra-articular condition of benign nature, characterised by villous proliferation of the synovium with replacement of subsynovial connective tissue by mature fat cells. It may be misdiagnosed as TGCT if encountered on fat-suppressed fluid-sensitive sequences and not correlated with a native T1-weighted sequence. However, its feathery subsynovial fat deposition appearance on axial MR images is characteristic (Fig. 6) [29]. The classic location is the suprapatellar recess of the knee joint. In most cases, lipoma arborescens does not extend to other recesses, except when it develops in patients with chronic synovitis, such as in rheumatoid or psoriatic arthritis.

Synovial haemangioma may cause repetitive spontaneous hemarthrosis within a joint and thereby mimic D-TGCT clinically. However, the MRI appearance with a “bag of worms” caused by serpentine vascular channels and the presence of interspersed fat in a haemangioma may be helpful to distinguish the two entities. In addition, the enhancement pattern differs and a dynamic post contrast sequence can be used to determine slow-flow versus high-flow vascularity in the synovial haemangioma [30]. Resection is the treatment of choice.

Haemophilic arthropathy may mimic D-TGCT due to widespread hemosiderin depositions and often severe secondary osteoarthritis; however, the clinical history is usually straightforward and fatty components are absent due to a lack of foam cells [18].

Treatment assessment in the knee

Pre- and postoperative MRI findings

Surgery is the mainstay of TGCT treatment, performed either open or arthroscopically [31]. L-TGCT resection is relatively straightforward, with low recurrence rates (4–30%) controlled by re-excision [32]. On the other hand, D-TGCT is a locally aggressive process with a high recurrence rate of around 40–60% [12, 33]. MRI is

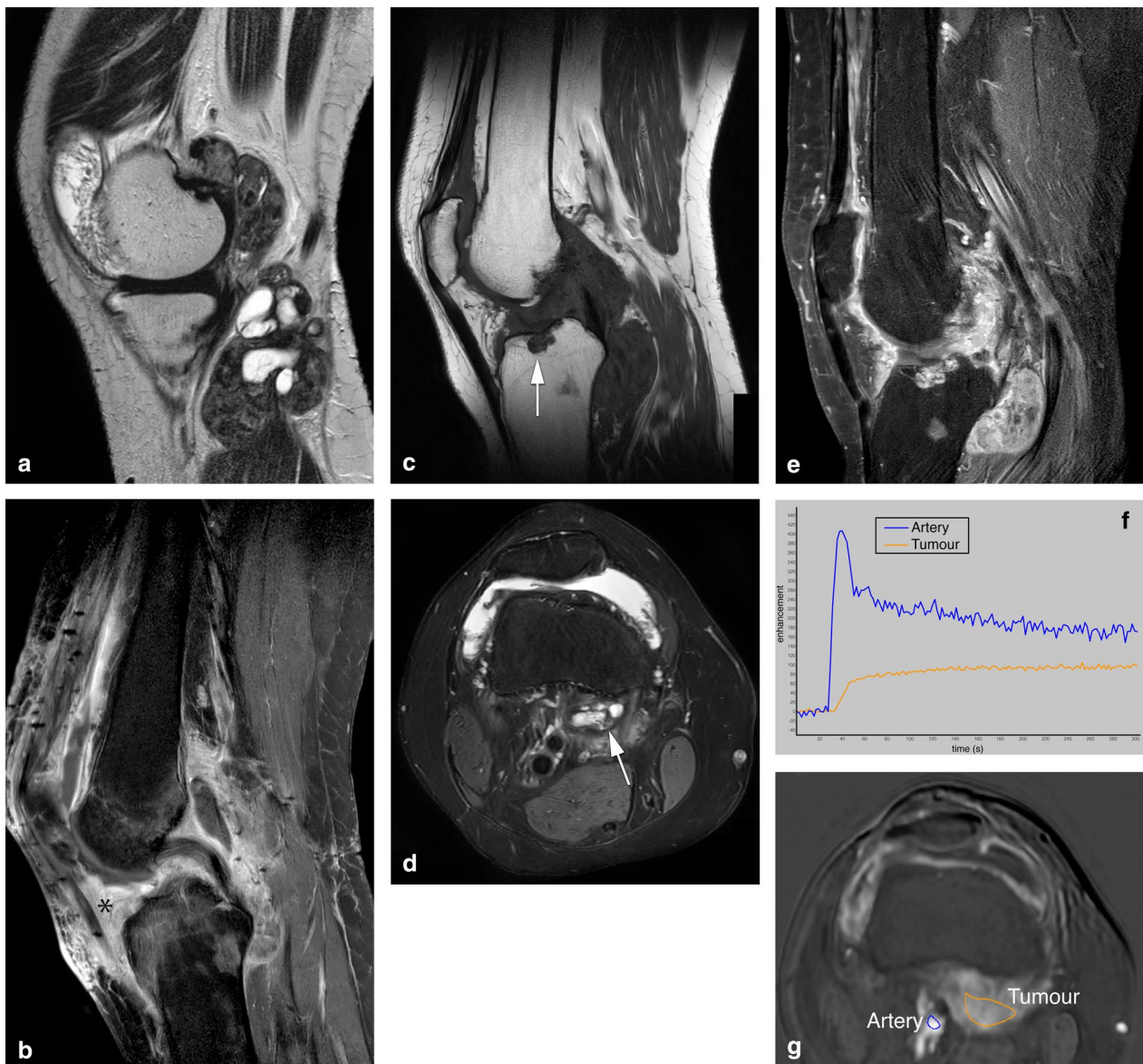


Fig. 2 A case of D-TGCT demonstrating pre and post synovectomy findings on MRI. **a** Sagittal T2 weighted image shows multilobular posterior tumour with low signal intensity, and adjacent cyst-like components present within tumour in the popliteal cyst. Anterior, in the medial gutter of the suprapatellar recess smaller synovial proliferations are present. **b** Sagittal T1 SPIR post contrast performed 3 months after anterior and posterior synovectomy shows surgical clips with metal artefact anterior and posterior in the soft tissues, thickening of the quadriceps tendon, subcutaneous oedema and marked enhancement in Hoffa's fatpad (asterisk) and along the posterior cortex of the tibia (subpopliteal recess). This mass-like enhancement can be post operative but residual tumour cannot be excluded at this time. *MRI performed 3 years post synovectomy*: **c** Sagittal T1 shows a bone erosion centrally in the tibial plateau (arrow). Furthermore, soft tissue masses posteriorly in the knee are present containing foci of low signal intensity. **d** Axial PD SPAIR shows a typical location of a lesion containing cystic components at the medial retrocondylar recess (arrow). **e** Sagittal T1 SPIR post contrast demonstrates enhancement of tumour within the tibia plateau erosion and of the posterior mass lesions. Note that Hoffa's fat pad shows normalisation of fatty signal intensity except for a rim of tumour enhancement in the central synovial recess and inferior infrapatellar recess. **f, g** Time intensity curve of the tumour based on the region of interest (orange line) of the lesion demonstrated in **d**, showing early enhancement within 10 s after the artery (blue line) followed by a plateau phase (type III curve suggestive of a benign lesion)

fundamental to assess D-TGCT intra- and extra-articular extension and can help avoid incomplete resections.

The knee joint intracapsular space is composed of multiple and interconnected synovial recesses, some

of which are rarely apparent on MRI of a healthy, non-affected knee [34]. D-TGCT is characteristically found in certain areas showing a reproducible distribution pattern similar to loose bodies [35]. Therefore,

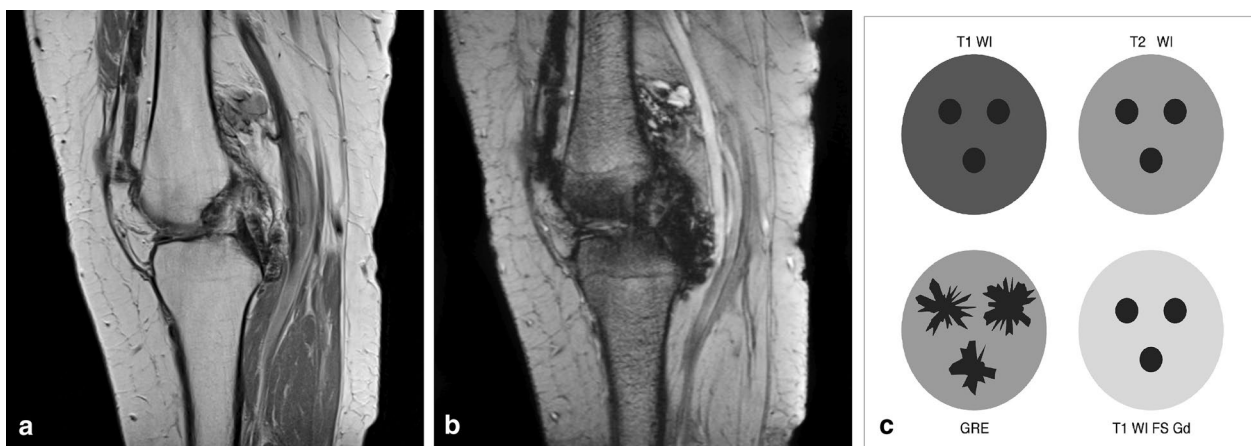


Fig. 3 Blooming artefact. **a** Sagittal PD-weighted MR image of the knee in a patient with D-TGCT demonstrates multiple low signal intensity synovial lesions posterior to the PCL, along the posterior cortex of the femoral metaphysis and in the collapsed suprapatellar recess. **b** Sagittal T2-weighted gradient echo MR image of the knee showing blooming artefact: the low signal intensity synovial lesions containing hemosiderin increase in size and are ill defined, appearing as cloud-like dark areas. **c** Schematic illustration of hemosiderin signal intensities on gradient echo (GRE) weighted sequences versus T1- and T2-weighted sequences. Gradient echo images show increased size of the hemosiderin foci with irregular margins, this is called "blooming"

D-TGCT lesions can be identified on MRI due to reactive joint effusion making synovial recesses apparent and due to signal intensity contrast between tumour and fluid.

The same MRI protocol should be used for pre- and post-treatment assessment (as described in Additional file 1: Table S1). Assessment of joint recesses may be done first in the sagittal plane (comparing T1-WI with T1-WI fat-suppressed (FS) gadolinium (Gd) side-to-side for anatomy and enhancement of lesions). Secondly, side-to-side comparison of axial fluid sensitive sequences (we use T2 DIXON) and T1-WI FS Gd images helps distinguish tumour from (rim-)enhancing synovial fluid or cyst-like components. Coronal images add value for assessment of erosions and femorotibial chondropathy.

The following areas should be carefully scrutinised and reported (Fig. 1):

The anterior compartment:

1. The suprapatellar recess is localised between the prefemoral and suprapatellar fat pads. It is the most distensible synovial recess, often containing hemosiderin deposits along its posterior synovial surface and nodular proliferations surrounded by joint fluid. Simultaneous assessment of T1-weighted images and fluid-sensitive sequences in axial and sagittal planes is crucial. The prefemoral fat has well-defined rounded margins, but not infrequently; it acquires dendritic borders protruding into the suprapatellar pouch resulting in TGCT overestimation due to taking fat-suppressed adipose tissue for TGCT.

The medial and lateral parapatellar gutters are key areas to assess on axial images because D-TGCT is frequently trapped here.

2. The infrapatellar synovial recess is divided into the superior and inferior recesses, orientated vertically and horizontally, respectively, including the localisation of tumour underneath the anterior horns of the menisci and the intermeniscal ligament.
3. The involvement of pre-patellar and infra-patellar bursae in D-TGCT is rare and should urge the investigation of other entities such as gout.

The posterior compartment has a limited distensible capacity defined by the posterior femoral capsule:

1. The subgastrocnemius synovial recesses, also referred to as retrocondylar or posterior femoral recesses, are localised underneath the gastrocnemius head insertions [35]. These areas present as fat signal intensity triangles with concave margins on sagittal T1-weighted images. Subgastrocnemius collapsed reactive synovitis without intervening effusion results in D-TGCT overestimation. Replacement of fat by low signal intensity tissue is in keeping with hemosiderin. Ganglion cysts at the medial or lateral gastrocnemius origins may be indistinguishable from tumour, because D-TGCT tends to show multiloculated thick-walled cystic masses [36]. The cleft-like morphology and presence of hemosiderin point towards D-TGCT, where it is prone to develop extra-



Fig. 4 Differential diagnosis: gout in the knee. **a** Lateral radiograph demonstrates marked pre-patellar soft tissue swelling containing increased density and several ill-defined calcifications (arrow). **b** Sagittal T1 shows a prepatellar, low signal intensity oval shaped soft tissue mass and a subchondral cyst in the patella. **c** Axial T2 FS confirms the prepatellar, low signal intensity mass invading the quadriceps tendon (arrows) and shows joint effusion containing multiple small synovial proliferations in the suprapatellar recess (asterisk). Aspiration of joint fluid with crystals confirmed the diagnosis of gout. **d** Axial T2 FS demonstrates low signal intensity soft tissue lesions in keeping with gout tophi deep to the collateral ligaments, causing erosion of the medial and lateral femoral condyles (arrows)

articular extension encasing the gastrocnemius tendons.

2. The PCL recess is located between the PCL and the posterior joint capsule. It usually harbours fibrofatty tissue with thin enhancing septa, which can be misdiagnosed as TGCT on fat-suppressed sequences [23]. The inspection of T1-weighted images and the absence of mass effect (posterior femoral capsule bulging) confirms its nature. This location is typical for extra-capsular D-TGCT popliteal extension due to perforating vessels on the posterior femoral capsule [37].
3. The subpopliteus synovial recess encases the popliteus tendon. It is connected to the popliteal hiatus between the posterosuperior and anteroinferior popliteomeniscal fascicles. It extends behind the posterior horn of the lateral meniscus to sit underneath the popliteus muscle belly in contact with the posterior aspect of the tibia. The subpopliteal recess represents a continuum with the proximal tibiofibular joint in approximately 10% of patients [38].
4. The Baker's or popliteal cyst is also known as the medial gastrocnemius—semimembranosus bursa. Baker's cyst D-TGCT involvement is considered



Fig. 5 Differential diagnosis: synovial chondromatosis in the knee. **a** Lateral radiograph illustrating multiple punctiform masses in the soft tissues of the knee containing speckled calcifications (arrows). These calcifications are present in Hoffa and posterior in the knee. **b** Sagittal T1 SPIR post contrast showing rim enhancement of the synovial lesions, which contain low signal intensity foci corresponding to the calcifications on X-ray. Only minimal joint effusion is present surrounding the cruciate ligaments with rim enhancement. **c** Axial T2 DIXON shows posterior extracapsular extension into the lateral head of gastrocnemius muscle (arrow)

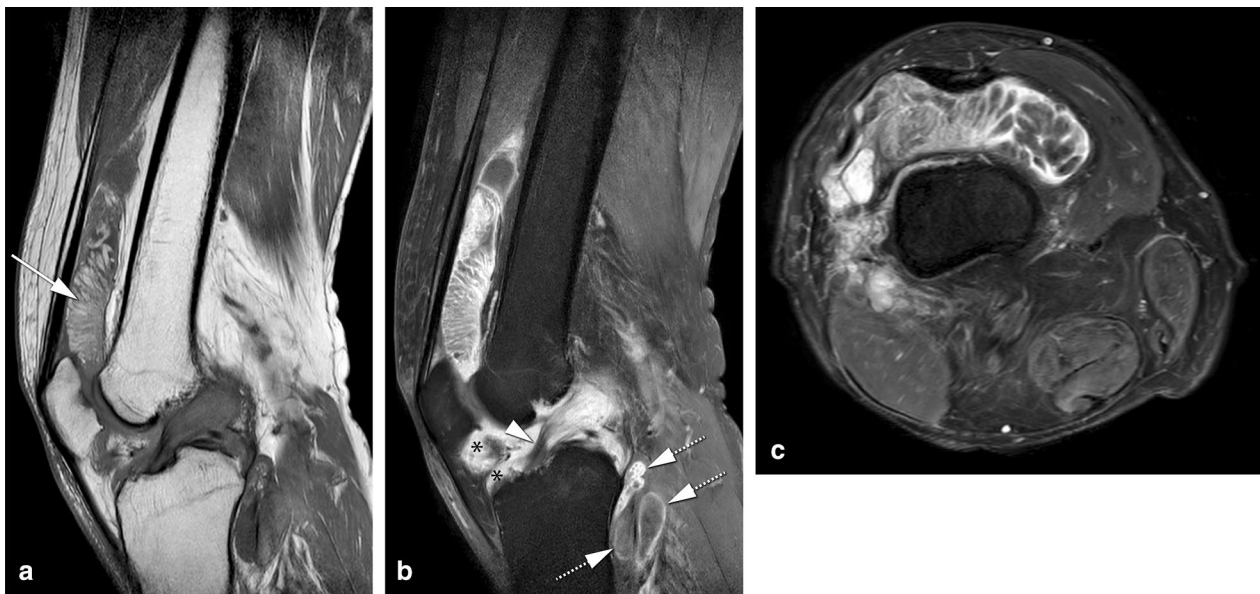


Fig. 6 Differential diagnosis: lipoma arborescens. **a** Sagittal T1 demonstrates a hyperintense soft tissue mass in the suprapatellar recess, containing multiple villous proliferations (arrow). **b** Sagittal T1 SPIR post contrast shows the signal of the villi is suppressed and rim enhancement is present. In addition, there is mucoid degeneration of the anterior cruciate ligament and enhancing synovitis in the central synovial recess (arrowhead), superior and inferior infrapatellar recesses (asterisks), PCL and subpopliteal recess (arrows). **c** Axial T2 DIXON confirms fat suppression of the villi in the suprapatellar recess. These findings are in keeping with a lipoma arborescens, which is not a true neoplasm but rather a reactive process associated with rheumatoid or psoriatic arthritis or osteoarthritis

intra-articular extension because of the communication with the knee joint synovial lining. Due to its dependent location and ball-valve communication mechanism, a Baker’s cyst can harbor multi-cystic proliferations with or without involvement of another

compartment. The medial gastrocnemius-semimembranosus tendon cross-over may mimic haemorrhage deposition, but its anti-gravitational site and axial tracking differentiate it from hemosiderin deposition.

5. Some bursae, such as the semimembranosus-tibial collateral ligament bursa (semimembranosus bursa) and pes anserinus are not connected to the knee joint and are atypical locations for D-TGCT.

The *middle compartment* is a tight area where distension is limited.

1. The central synovial recess is situated in front of the ACL.
2. The intercruciate space is challenging to assess on MRI, as D-TGCT is generally underestimated in this area due to the similar low signal intensity compared to the cruciate ligaments. Intra-articular pericruciate ganglion cysts should be differentiated from tumour. Bone erosions caused by the tumour in the intercondylar notch can be undercalled as cystic change at the insertion of the cruciate ligaments, which is a common finding on normal knee MRIs [39]. Bone erosions in D-TGCT typically contain enhancing tumour tissue (Fig. 2C, E).
3. The femorotibial synovial recesses, both medial and lateral, are occupied in severe D-TGCT cases when tumour volume generally exceeds 80–100 cc. These areas are prone to develop cortical erosions as they are virtually not distensible.

MRI is the modality of choice to assess residual D-TGCT after synovectomy and for postoperative follow-up. Common postoperative changes include skin thickening, fat stranding or inflammation in Hoffa (in the area of arthroscopy portal entrances), subcutaneous and intramuscular oedema with susceptibility artefacts secondary to surgical clips (Fig. 2B). Joint effusion may be reduced due to drainage. Diffuse synovial thickening is equivocal for D-TGCT residual disease within the first six months because of associated reactive synovitis [40]. Growing enhancing solid and nodular synovial thickening should raise the suspicion of disease recurrence (Fig. 2B, E).

Systemic therapy response evaluation

With the arrival of systemic therapies targeting CSF1/CSF1R in D-TGCT patients not regarded amenable to surgery, MRI is required to objectively assess treatment response [16, 17, 41]. Quantification of change in tumour volume is the main feature to evaluate the response of these agents. To date, Response Evaluation Criteria in Solid Tumours (RECIST) 1.1 is the most frequently used tool to detect a change in tumour size by calculating the sum of the longest diameters for all target lesions. In addition, a modification of RECIST (m-RECIST) can be applied, adding a short axis measurement for target

lesions, offering higher accuracy [17]. However, the irregular tumour shape, absence of nodular lesions, asymmetrical growth, variable enhancement after contrast, and lack of clear tumour margins make it challenging to apply linear measurements [42].

Peterfy et al. developed a semiquantitative, joint-specific, visual tumour volume score (TVS) for D-TGCT. This score was developed analogous to and based on arthritis visual scores used in clinical trials. TVS expresses tumour volume as a percentage of the estimated volume of the maximally distended normal synovial cavity of the involved joint. TVS can incorporate all tumour regions and defines tumour size relative to the joint size [42]. However, since TVS is a semiquantitative tool, clinicians have to estimate the percentage of tumour volume, limiting its reproducibility. In addition, TVS has not been validated as a method for response assessment yet. Therefore, there is an urgent need for an automated tool measuring D-TGCT tumour volume on MRI.

Aside from changes in tumour size, other specific MRI findings following CSF1R inhibitors have been described in pilot studies. These findings include a decrease in signal intensity on fluid-sensitive sequences with a reduction of capsular distension and joint effusion and an increase in hemosiderin deposition [43]. Decreased enhancement seems to be an equivocal parameter. These imaging features appear to correlate well with clinical improvements, such as pain reduction (Fig. 7) [44].

Of note, patients may experience complete symptomatic relief even in the setting of what appears to be an incomplete response based on imaging [43]. So-called hemosiderin scars remain as a low signal intensity rim lining the synovium after therapy, without corresponding clinical complaints. It has been suggested to use “complete response” in case of residual hemosiderin scars with a short axis < 5 mm, however this approach needs further study [42].

Future directions: 3D segmentation

Following the limitations of the current response criteria, volumetric quantification techniques integrated with Artificial Intelligence (especially deep learning) methods may help measure tumour change. However, developing such an automated quantification method is challenging due to irregular growth and heterogeneous signal intensity of TGCT [42].

We performed a first step towards objective volumetric quantification of D-TGCT by segmenting 3D tumour volume in 40 treatment-naïve patients with D-TGCT. All imaging data were anonymised, and informed consent was waived by the institutional review board (G19.127). Measuring tumour volume was done in Brainlab

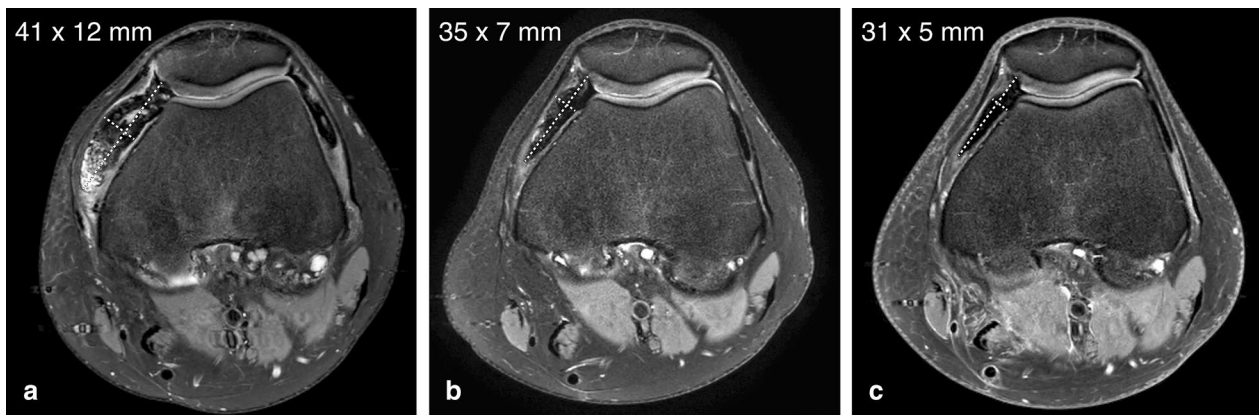


Fig. 7 MRI findings after treatment of D-TGCT with a CSF1R inhibitor. **a** Axial PD SPAIR images in a patient with intra-articular D-TGCT. Baseline image showing a target lesion (two axial diameters measured according to modified RECIST, dotted lines) in the medial suprapatellar recess. Note a smaller similar lesion in the lateral suprapatellar recess. **b** After 8 weeks on CSF1R-inhibitor therapy, the tumour showed a significant decrease in size and signal intensity. Joint effusion was resolved (not shown). The patient experienced improvement in symptoms of pain and swelling. **c** After 36 weeks, residual low signal intensity hemosiderin “scars” remained both in the medial and lateral suprapatellar recesses

(Elements), an application that is commonly used for pre-operative planning of bone and soft-tissue tumours.

For 3D segmentation, a sagittal T1 spectral inversion recovery (SPIR) Gd and an axial T2 DIXON (water only) scan were utilised. In addition to the total volume, the volumes in the anterior and posterior compartments of

the knee were calculated separately. The mean total volume was 44 cm^3 (range $3.2\text{--}208.8 \text{ cm}^3$). The mean volume located in the anterior compartment was 21 cm^3 (range $0.0\text{--}205.8 \text{ cm}^3$) and in the posterior compartment 23 cm^3 (range $0.0\text{--}172.9 \text{ cm}^3$). Examples of

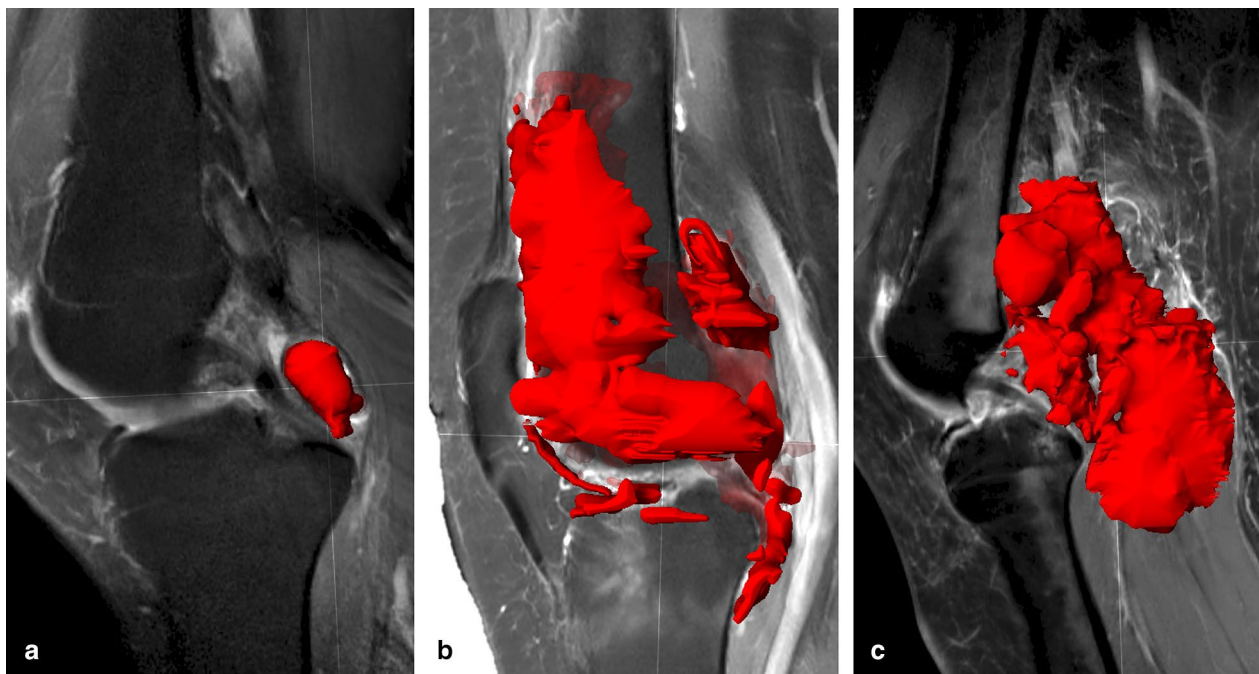


Fig. 8 Volumetric segmentations of D-TGCT performed with Brainlab software on sagittal T1 SPIR-weighted sequences post gadolinium. **a** Tumour is segmented in the PCL recess (volume shown in red). Volume: 3.8 cm^3 . **b** Tumour segmentation in anterior, middle and posterior compartments. Volume: 86.2 cm^3 . **c** Tumour segmentation of a case with marked posterior disease, present in the PCL recess, subgastrocnemius synovial recesses, Baker's cyst, and extending extra-articular in the popliteal fossa. Volume: 91.9 cm^3

Table 1 D-TGCT Knee MRI structured report template

Items	Findings
1. Shape	Well-circumscribed nodules <i>and/or</i> diffuse villous synovial thickening
2. Site	
2a. Intra-articular	Anterior compartment (suprapatellar, superior and inferior infrapatellar recesses) Middle compartment (central, femorotibial, intercruciate recesses) Posterior compartment (retrocondylar, PCL, subpopliteus, Baker's cyst) Cartilage and bone invasion by the tumour (tumour extension in pressure erosions)
2b. Extra-articular	Posterior transcapsular extension to popliteal fossa Muscular-tendinous involvement (invasion or encasement > 180°) Ligament involvement (invasion or encasement > 180°) Neurovascular bundle involvement (> 180° encasement of the tibial nerve and/or popliteal artery/veins)
3. Signal intensity	T1-WI: (hypo-/isointense) and (homogeneous/heterogeneous) T2-WI FS: (hypo-/iso-/hyperintense) and (homogeneous/heterogeneous) T1-WI FS Gd: enhancement (absent/present) and (homogeneous or heterogeneous) T2*-WI or T1 GRE: blooming (absent/present)
4. Size	Bidimensional measurements [RECIST 1.1: long axis of target lesions, modified RECIST: long and short axis of target lesions] Volumetric tumour burden (Tumour Volume Score)
5. Secondary findings (complications)	Joint Effusion (> 10 mm anteroposterior in the suprapatellar pouch) Reactive synovitis (sometimes fatty metaplasia, hyperintense on T1-WI) Secondary osteoarthritis/Chondromalacia
Conclusion	
Subtype (growth pattern)	Diffuse-type TGCT (≥ 2 synovial recesses)
Extension	Intra-articular and/or extra-articular
Complications	Secondary osteoarthritis (mild, moderate, severe)

PCL, posterior cruciate ligament; WI, weighted imaging; FS, fat-suppressed; Gd, gadolinium; GRE, gradient echo; RECIST, response evaluation criteria in solid tumours

volumetric segmentation in three different patients are shown in Fig. 8.

We showed that 3D MR segmentation allows to objectively quantify the tumour burden of TGCT and provides a quick visual assessment of TGCT lesion distribution throughout the knee. However, since 3D segmentation of TGCT is time-consuming and operator-dependent, future steps will focus on automating this process.

Conclusions

MRI is the modality of choice in diagnosing D-TGCT, providing preoperative mapping and assessment of response to systemic therapies. However, due to its irregular shape, extensive growth and low signal intensity, D-TGCT disease extent can be challenging for the radiologist. We highlighted imaging characteristics of D-TGCT affecting the knee and provided a structured report template (Table 1). In addition, pitfalls such as mimickers of D-TGCT were addressed, and evaluation of tumour response following new systemic therapies. Finally, we demonstrated a first step towards objective 3D volume quantification of D-TGCT. Automated quantification of tumour load to assess treatment response will become more important as systemic medical therapies evolve quickly.

Abbreviations

ACL	Anterior cruciate ligament
ADC	Apparent diffusion coefficient
Ax	Axial
Cor	Coronal
CSF1	Colony-stimulating factor 1
CSF1R	Colony-stimulating factor 1-receptor
CT	Computed tomography
D-TGCT	Diffuse-type tenosynovial giant cell tumour
DWI	Diffusion-weighted images
FFE	Fast field echo
FOV	Field-of-view
FS	Fat-suppressed
Gd	Gadolinium
GRE	Gradient echo
IR	Inversion recovery
L-TGCT	Localised-type tenosynovial giant cell tumour
m-RECIST	Modification of RECIST
MRI	Magnetic Resonance Imaging
MST	Multi-stack
PCL	Posterior cruciate ligament
PD	Proton density
RECIST	Response evaluation criteria in solid tumours
Sag	Sagittal
SE	Spin-echo
SP(A)IR	Spectral (adiabatic) recovery
TFE	Turbo field echo
TGCT	Tenosynovial giant cell tumour
TSE	Turbo spin echo
TVS	Tumour volume score
WI	Weighted imaging

Supplementary Information

The online version contains supplementary material available at <https://doi.org/10.1186/s13244-023-01367-z>.

Additional file 1: Table S1. MRI protocol for D-TGCT of the knee.

Acknowledgements

We want to thank Gerrit Kracht for his contribution to the figures in this manuscript.

Author contributions

GS: conceptualisation, investigation, data-curation, writing-original draft, writing-review and editing. CS: investigation, segmentation of tumours in Brainlab, formal analysis, writing-original draft, writing-review and editing. BS: data-curation, methodology, formal analysis, writing-review and editing. AC: data curation, writing-review and editing. HG: supervision, writing-review and editing. MvdS: data curation, supervision, writing-review and editing. KVL: conceptualisation, investigation, formal analysis, supervision, writing-original draft, writing-review and editing. All authors read and approved the final manuscript.

Funding

Not applicable.

Availability of data and materials

Not applicable.

Declarations

Ethics approval and consent to participate

All imaging data were anonymised, and informed consent was waived by the institutional review board (G19.127).

Consent for publication

Not applicable.

Competing interests

GS and MvdS report research funding from Daiichi-Sankyo to their department outside this submitted work.

Author details

¹Department of Orthopaedic Surgery, Leiden University Medical Centre, Postzone J11-R-70, PO Box 9600, 2300 RC Leiden, The Netherlands. ²Department of Radiology, Hospital Universitario Ramón y Cajal, Madrid, Spain. ³Division of Image Processing, Department of Radiology, Leiden University Medical Centre, Leiden, The Netherlands. ⁴Department of Radiology, Leiden University Medical Centre, Leiden, The Netherlands. ⁵Department of Medical Oncology, Leiden University Medical Centre, Leiden, The Netherlands.

Received: 10 August 2022 Accepted: 3 January 2023

Published online: 01 February 2023

References

- de St. Aubain Somerhausen N, Van de Rijn M (2020) Tenosynovial giant cell tumour. In: WCoTEB (ed) 5th World Health Organization Classification of Tumours of Soft Tissue and Bone. IARC Press, Lyon
- Gelhorn HL, Tong S, McQuarrie K et al (2016) Patient-reported symptoms of tenosynovial giant cell tumors. *Clin Ther* 38(4):778–793
- Murphey MD, Rhee JH, Lewis RB, Fanburg-Smith JC, Flemming DJ, Walker EA (2008) Pigmented villonodular synovitis: radiologic-pathologic correlation. *Radiographics* 28(5):1493–1518
- Sciot R, Rosai J, Dal Cin P et al (1999) Analysis of 35 cases of localized and diffuse tenosynovial giant cell tumor: a report from the Chromosomes and Morphology (CHAMP) study group. *Mod Pathol* 12(6):576–579
- Mastboom MJL, Verspoor FGM, Verschoor AJ et al (2017) Higher incidence rates than previously known in tenosynovial giant cell tumors. *Acta Orthop* 88(6):688–694
- Ehrenstein V, Andersen SL, Qazi I et al (2017) Tenosynovial giant cell tumor: incidence, prevalence, patient characteristics, and recurrence. A registry-based cohort study in Denmark. *J Rheumatol* 44(10):1476–1483
- Ushijima M, Hashimoto H, Tsuneyoshi M, Enjoji M (1986) Giant cell tumor of the tendon sheath (nodular tenosynovitis). A study of 207 cases to compare the large joint group with the common digit group. *Cancer* 57(4):875–884
- Kim DE, Kim JM, Lee BS, Kim NK, Lee SH, Bin SI (2018) Distinct extra-articular invasion patterns of diffuse pigmented villonodular synovitis/tenosynovial giant cell tumor in the knee joints. *Knee Surg* 26(11):3508–3514
- Nishida Y, Tsukushi S, Nakashima H et al (2012) Osteochondral destruction in pigmented villonodular synovitis during the clinical course. *J Rheumatol* 39(2):345–351
- West RB, Rubin BP, Miller MA et al (2006) A landscape effect in tenosynovial giant-cell tumor from activation of CSF1 expression by a translocation in a minority of tumor cells. *Proc Natl Acad Sci U S A* 103(3):690–695
- Barile A, Sabatini M, Iannessi F et al (2004) Pigmented villonodular synovitis (PVNS) of the knee joint: magnetic resonance imaging (MRI) using standard and dynamic paramagnetic contrast media. Report of 52 cases surgically and histologically controlled. *Radiol Med* 107(4):356–366
- Mastboom MJL, Palmerini E, Verspoor FGM et al (2019) Surgical outcomes of patients with diffuse-type tenosynovial giant-cell tumours: an international, retrospective, cohort study. *Lancet Oncol* 20:877–886
- Spierenburg G, van der Heijden L, Mastboom MJL et al (2022) Surgical management of 144 diffuse-type TGCT patients in a single institution: a 20-year cohort study. *J Surg Oncol* 126:1087–1095
- Gortzak Y, Vitenberg M, Frenkel Rutenberg T et al (2018) Inconclusive benefit of adjuvant (90)Yttrium hydroxyapatite to radiosynovectomy for diffuse-type tenosynovial giant-cell tumour of the knee. *Bone Joint J* 100-B(7):984–988
- Mollon B, Lee A, Busse JW et al (2015) The effect of surgical synovectomy and radiotherapy on the rate of recurrence of pigmented villonodular synovitis of the knee: an individual patient meta-analysis. *Bone Joint J* 97-B(4):550–557
- Gelderblom H, Cropet C, Chevreau C et al (2018) Nilotinib in locally advanced pigmented villonodular synovitis: a multicentre, open-label, single-arm, phase 2 trial. *Lancet Oncol* 19(5):639–648
- Tap W (2020) ENLIVEN study: pexidartinib for tenosynovial giant cell tumor (TGCT). *Future Oncol* 16(25):1875–1878
- Hughes TH, Sartoris DJ, Schweitzer ME, Resnick DL (1995) Pigmented villonodular synovitis: MRI characteristics. *Skeletal Radiol* 24(11):7–12
- Pope TL Jr (2013) Aunt Minnie's Atlas and Imaging-specific diagnosis. Lippincott Williams & Wilkins
- McKee TC, Belair JA, Sobol K, Brown SA, Abraham J, Morrison W (2020) Efficacy of image-guided synovial biopsy. *Skeletal Radiol* 49(6):921–928
- Bassetti E, Candreva R, Santucci E (2011) Pigmented villonodular synovitis of the knee: a case report. *J Ultrasound* 14(3):167–169
- Mastboom MJL, Verspoor FGM, Hanff DF et al (2018) Severity classification of tenosynovial giant cell tumours on MR imaging. *Surg Oncol* 27(3):544–550
- Crim J, Dyroff SL, Stensby JD, Evenski A, Layfield LJ (2021) Limited usefulness of classic MR findings in the diagnosis of tenosynovial giant cell tumor. *Skeletal Radiol* 50:1585–1591
- Ashikyan O, Chalian M, Moore D, Xi Y, Pezeshk P, Chhabra A (2019) Evaluation of giant cell tumors by diffusion weighted imaging-fractional ADC analysis. *Skeletal Radiol* 48(11):1765–1773
- Drapé JL (2013) Advances in magnetic resonance imaging of musculoskeletal tumours. *Orthop Traumatol Surg Res* 99(1 Suppl):S115–S123
- Narváez JA, Narváez J, Ortega R, De Lama E, Roca Y, Vidal N (2003) Hypointense synovial lesions on T2-weighted images: differential diagnosis with pathologic correlation. *AJR Am J Roentgenol* 181(3):761–769
- Finkelstein D, Foremny G, Singer A et al (2021) Differential diagnosis of T2 hypointense masses in musculoskeletal MRI. *Skeletal Radiol* 2021(50):1981–1994
- Davies J, Riede P, van Langevelde K, Teh J (2019) Recent developments in advanced imaging in gout. *Ther Adv Musculoskelet Dis* 11:1759720x19844429

29. Wadhwa V, Cho G, Moore D, Pezeshk P, Coyner K, Chhabra A (2016) T2 black lesions on routine knee MRI: differential considerations. *Eur Radiol* 26(7):2387–2399
30. Rudd A, Pathria MN (2022) Intra-articular neoplasms and masslike lesions of the knee: emphasis on MR imaging. *Magn Reson Imaging Clin N Am* 30(2):339–350
31. Healey JH, Bernthal NM, van de Sande M (2020) Management of tenosynovial giant cell tumor: a neoplastic and inflammatory disease. *J Am Acad Orthop Surg Glob Res Rev* 4(11):e2000028
32. Mastboom MJL, Staals EL, Verspoor FGM et al (2019) Surgical treatment of localized-type tenosynovial giant cell tumors of large joints: a study based on a multicenter-pooled database of 31 international sarcoma centers. *J Bone Joint Surg Am* 101(14):1309–1318
33. Palmerini E, Staals EL, Maki RG et al (2015) Tenosynovial giant cell tumour/pigmented villonodular synovitis: outcome of 294 patients before the era of kinase inhibitors. *Eur J Cancer* 51(2):210–217
34. Bolog NV, Andreisek G, Ulbrich EJ (2015) Synovium and capsule. MRI of the knee. Springer, pp 137–167
35. Gursoy M, Mete BD, Dag F, Bulut T (2019) The distribution of loose bodies determined on knee magnetic resonance imaging: joint compartments, recesses and bursae including arthroscopic blind spots. *Acta Radiol* 60(10):1286–1293
36. James SL, Connell DA, Bell J, Saifuddin A (2007) Ganglion cysts at the gastrocnemius origin: a series of ten cases. *Skeletal Radiol* 36(2):139–143
37. Saifuddin A, Tyler P, Hargunani R (2016) Musculoskeletal MRI. CRC Press
38. Fenn S, Datir A, Saifuddin A (2009) Synovial recesses of the knee: MR imaging review of anatomical and pathological features. *Skeletal Radiol* 38(4):317–328
39. Bergin D, Morrison WB, Carrino JA, Nallamshetty SN, Bartolozzi AR (2004) Anterior cruciate ligament ganglia and mucoid degeneration: coexistence and clinical correlation. *AJR Am J Roentgenol* 182(5):1283–1287
40. Kassirjian A, Rubin DA (2021) Postoperative knee and shoulder. *Musculoskeletal Diseases 2021–2024*:121–138
41. Cassier PA, Italiano A, Gomez-Roca C et al (2020) Long-term clinical activity, safety and patient-reported quality of life for emactuzumab-treated patients with diffuse-type tenosynovial giant-cell tumour. *Eur J Cancer* 141:162–170
42. Peterfy C, Chen Y, Countryman P et al (2022) CSF1 receptor inhibition of tenosynovial giant cell tumor using novel disease-specific MRI measures of tumor burden. *Future Oncol* 18:1449–1459
43. Helming A, Hansford B, Beckett B (2022) Tenosynovial giant cell tumor-diffuse type, treated with a novel colony-stimulating factor inhibitor, pexidartinib: initial experience with MRI findings in three patients. *Skeletal Radiol* 51:1085–1091
44. Van De Sande M, Tap WD, Gelhorn HL et al (2021) Pexidartinib improves physical functioning and stiffness in patients with tenosynovial giant cell tumor: results from the ENLIVEN randomized clinical trial. *Acta Orthop* 12:1–7

Publisher's Note

Springer Nature remains neutral with regard to jurisdictional claims in published maps and institutional affiliations.

Submit your manuscript to a SpringerOpen[®] journal and benefit from:

- Convenient online submission
- Rigorous peer review
- Open access: articles freely available online
- High visibility within the field
- Retaining the copyright to your article

Submit your next manuscript at ► [springeropen.com](https://www.springeropen.com)
